

Supporting info for:
 Antibody-Mediated Self-Limiting Self-Assembly for Quantitative Analysis
 of Nanoparticle Surfaces by Atomic Force Microscopy

Carly Lay A. Geronimo, Robert I. MacCuspie

Initial AuNP stocks characterization.

For 10 nm AuNPs, the particles were found to have a Z-average of (17.0 ± 0.2) nm. The initial UV-Vis spectrum for 10 nm AuNPs with a maximum absorbance at a wavelength of 518 nm. 60 nm AuNPs exhibited a Z-average of (58.2 ± 0.2) nm. The initial UV-Vis spectrum for 60 nm AuNPs with a maximum absorbance at a wavelength of 528 nm. Small differences were noted between the values observed here and the reference values provided with the NIST Reference Material Certificates, (13.5 ± 0.1) nm and (56.6 ± 1.4) nm for the nominally 10 nm and 60 nm AuNPs, respectively. These differences are likely due to experimental differences which may include using different algorithms and fitting constraints to analyze the correlation functions, using disposable semi-micro cuvettes (which can artificially introduce errors from scattering due to the geometry of the plastic cuvette) instead of quartz cuvettes, and perhaps physical modification to or agglomeration of the AuNPs as a consequence of the syringe filtration processing step.

Table SI-1. Reaction conditions for Antibody functionalization onto AuNPs.

Sample	AuNP diam.	Ab / NP	Volume of MPA	Volume of NHS	Volume of EDAC	Volume of Antibody
1, 4, 7	60nm	1	38.0 μL of $1.1 \text{ nmol}\cdot\text{L}^{-1}$	49.6 μL of $0.87 \text{ nmol}\cdot\text{L}^{-1}$	1.66 μL of $52 \text{ nmol}\cdot\text{L}^{-1}$	$64.8 \mu\text{L}$ of $10^{-4} \text{ mg}\cdot\text{mL}^{-1}$ Ab
2, 5, 8	60nm	2	76.0 μL of $1.1 \text{ nmol}\cdot\text{L}^{-1}$	99.2 μL of $0.87 \text{ nmol}\cdot\text{L}^{-1}$	3.32 μL of $52 \text{ nmol}\cdot\text{L}^{-1}$	$129.6 \mu\text{L}$ of $10^{-4} \text{ mg}\cdot\text{mL}^{-1}$ Ab
3, 6, 9	60nm	10	380 μL of $1.1 \text{ nmol}\cdot\text{L}^{-1}$	4.96 μL of $87 \text{ nmol}\cdot\text{L}^{-1}$	16.6 μL of $52 \text{ nmol}\cdot\text{L}^{-1}$	$6.48 \mu\text{L}$ of $10^{-2} \text{ mg}\cdot\text{mL}^{-1}$ Ab
10	10nm	1	83.4 μL of $115 \text{ nmol}\cdot\text{L}^{-1}$	109 μL of $87 \text{ nmol}\cdot\text{L}^{-1}$	364 μL of $52 \text{ nmol}\cdot\text{L}^{-1}$	$142 \mu\text{L}$ of $10^{-2} \text{ mg}\cdot\text{mL}^{-1}$ Rabbit anti-Goat IgG
11	10nm	1	83.4 μL of $115 \text{ nmol}\cdot\text{L}^{-1}$	109 μL of $87 \text{ nmol}\cdot\text{L}^{-1}$	364 μL of $52 \text{ nmol}\cdot\text{L}^{-1}$	$142 \mu\text{L}$ of $10^{-2} \text{ mg}\cdot\text{mL}^{-1}$ Goat anti-Rabbit IgG
12	10nm	1	83.4 μL of $115 \text{ nmol}\cdot\text{L}^{-1}$	109 μL of $87 \text{ nmol}\cdot\text{L}^{-1}$	364 μL of $52 \text{ nmol}\cdot\text{L}^{-1}$	$142 \mu\text{L}$ of $10^{-2} \text{ mg}\cdot\text{mL}^{-1}$ Donkey anti-Rabbit IgG

Table SI-1. Specified volume and concentration of MPA, NHS, EDAC, and Antibody. Rabbit anti-Goat IgG was used for samples 1-3, Goat anti-Rabbit IgG was used for samples 4-6, and Donkey anti-Rabbit IgG was used for samples 7-9.

Kinetics of Self-Limiting Self-Assembly at 37 °C observed by DLS.

The self-assembly of the 10 nm AuNPs onto the 60 nm AuNPs was observed by DLS at the physiological temperature of 37 °C. Figure SI-1 shows the Z_{avg} over time for the self-assembly of 60 nm AuNP-Rabbit anti-Goat IgG (2 Lig/NP) with 10nm AuNP-**Ab** (1 Ab/NP), with **Ab** representing the two Ab's used including Goat anti-Rabbit IgG and Donkey anti-Rabbit IgG. The peak mean intensity was measured for the 60 nm Ab AuNP before addition of 10 nm AuNPs at time 0 s and for 2640 s afterwards in 120 s intervals. For Goat anti-Rabbit IgG, the structures exhibited a Z_{avg} increase of 20.3 nm, while the Donkey anti-Rabbit IgG containing structures increased by 19.4 nm. The absolute increase here is surprisingly large based on geometrical predictions of the Z_{avg} increase, suggesting that the hydrodynamic envelope being measured may include significant amounts of solvent associated with the raspberry-like particles. Figure SI-1 also shows the results for the self-assembly of 60 nm AuNP-Rabbit anti-Goat IgG (10 Lig/NP) with 10 nm AuNP-**Ab** (1 Ab/NP). For Goat anti-Rabbit IgG, the structures exhibited a measurement increase of 27.3 nm, while for Donkey anti-Rabbit IgG an increase of 26.0 nm was observed. Based on the data, Goat anti-Rabbit IgG showed a greater Z_{avg} increase, perhaps because it expressed a reciprocated affinity with Rabbit anti-Goat IgG, or perhaps due to subtle size differences in IgG molecules from species to species. While increasing the Lig/NP of the 60 nm AuNP expressed a greater Z_{avg} increase, it was not on the order of what would be predicted from the solution synthesis stoichiometry, which agrees with the AFM observations. Also of interest, the kinetics of the self-assembly reactions were nearly identical whether 2 Ab/NP or 10 Ab/NP, suggesting standardization of the self-limiting self-assembly time to less than 30 min is possible.

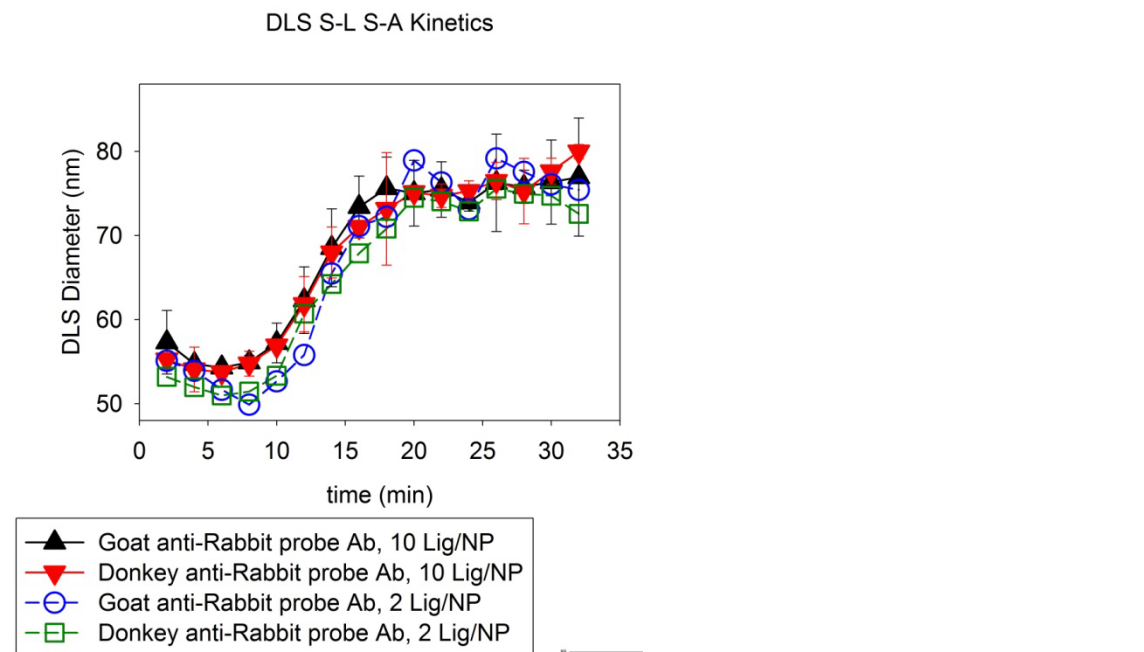


Figure SI-1. Kinetics of self-limiting self-assembly of raspberry-like structures. Points are the mean of three measurements, with uncertainty bars representing one standard deviation of the mean.

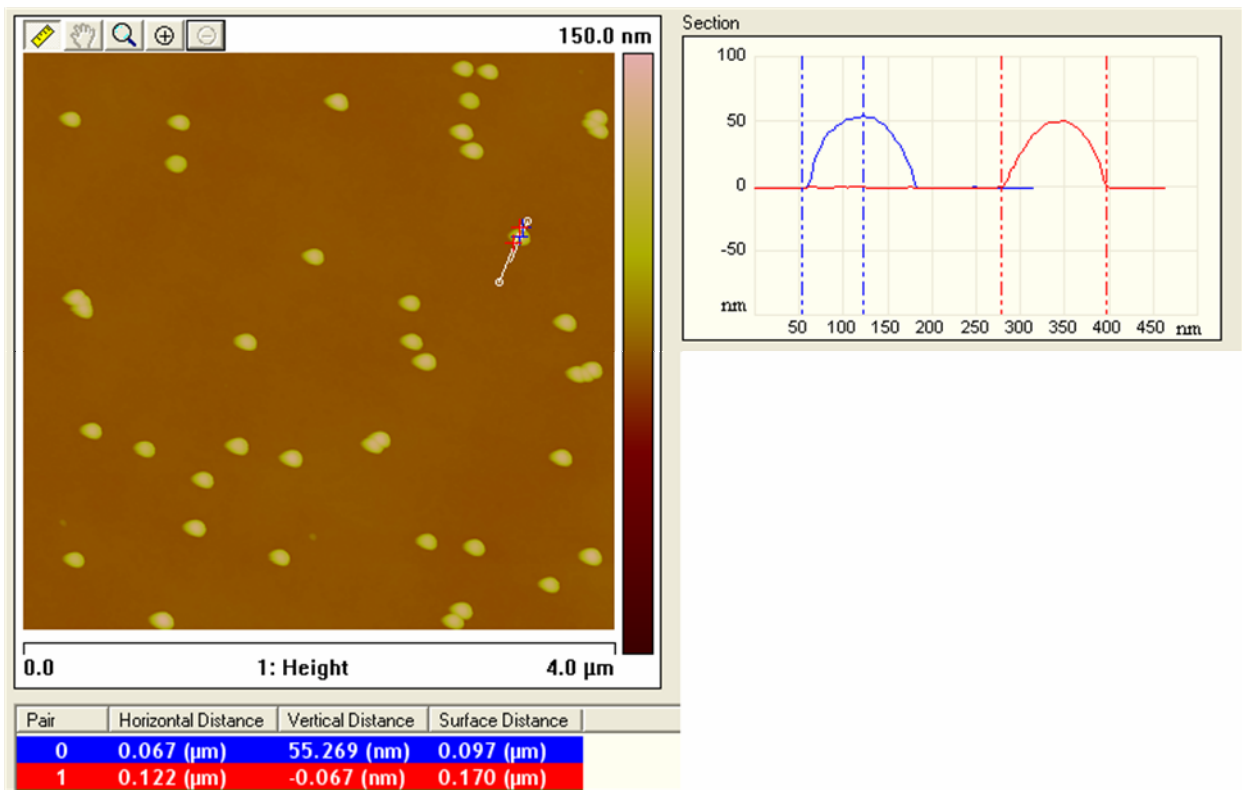


Figure SI-2. Screenshot of cross-section analysis of nominally 60 nm AuNPs used to estimate the tip radius of curvature.

Using the method described in Markiewicz & Goh, Langmuir, 1994, assuming spherical geometries for both the AFM tip and the surface structure, the equation $d=w^2/4h$ can be applied where d is the diameter of the AFM tip, w is the apparent measured width of the structure (includes the tip broadening effect), and h is the measured height of the structure. Using the data from Figure SI-2 as an example, $w = 170$ nm, $h = 55.3$ nm, and thus the tip radius of curvature employed in this experiment was 65 nm. While this is much broader than the vendor reported tip radius of curvature, it does not impact the shape of a cross-section analysis of a raspberry-like structure, as seen later in Figure SI-8.

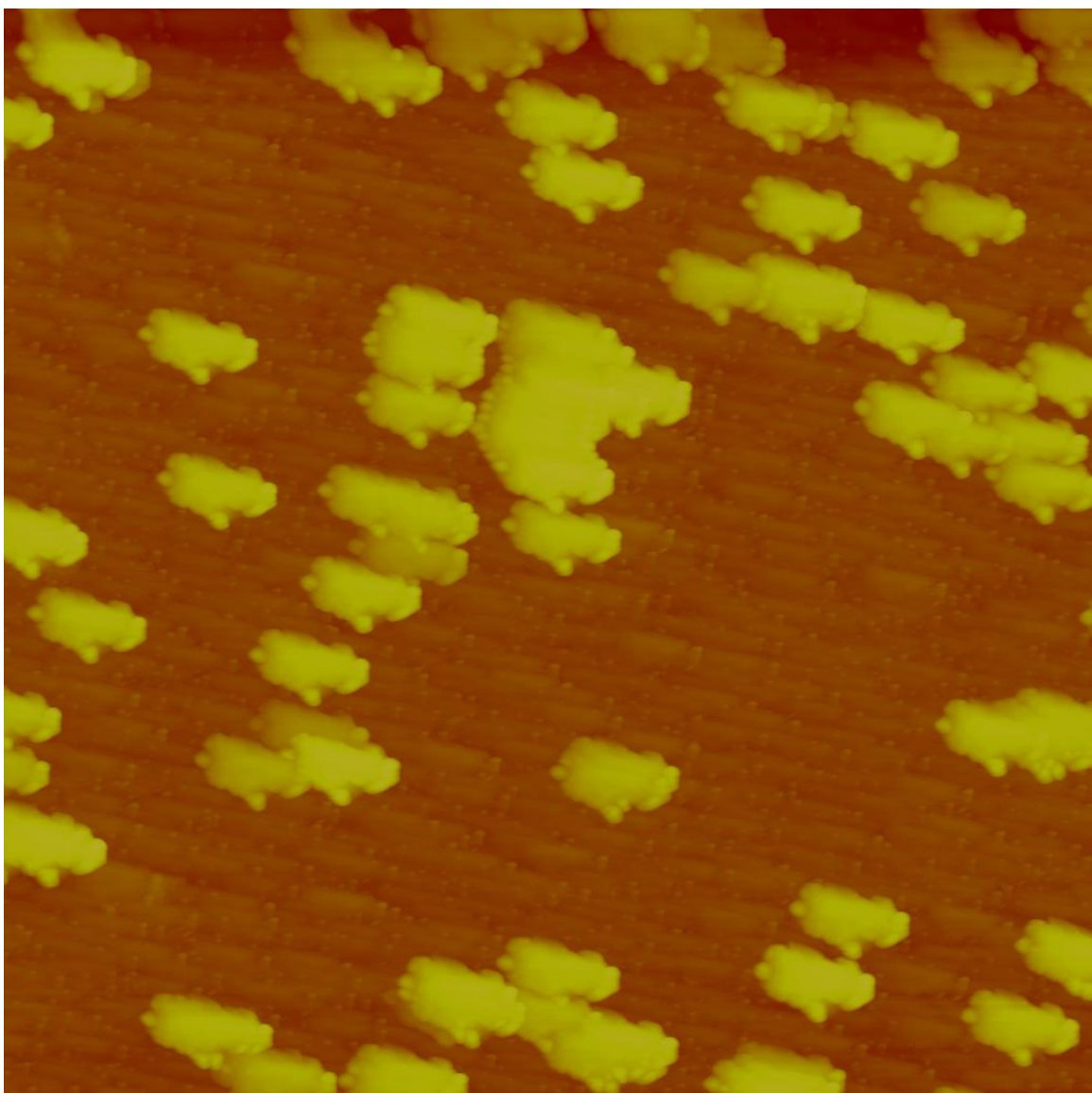


Figure SI-3. Image collected with a damaged or contaminated tip of neat AuNPs. Notice the repetitive unusual morphology of every particle, especially compared to the morphology of the raspberry-like self-limiting self-assemblies such as in Figures 3 and 4 and Figures SI-3 to SI-6.

Calculation of predicted hydrodynamic diameter size increase

Assuming an IgG molecule, or antibody (Ab) has a hydrodynamic diameter of 14 nm (<http://www.nature.com/nature/journal/v445/n7129/full/nature05532.html>), and assuming simple volume addition,

$$V_{tot} = V_{NP} + (N_{Ab} \times V_{Ab})$$

where V_{tot} is the total volume, V_{NP} is the volume of the nanoparticle, N_{Ab} is the number of antibodies attached to the surface of the nanoparticle, and V_{Ab} is the volume of an antibody. Similarly, by simple volume addition, an equivalent DLS Z_{avg} size increase can be calculated for the self-limiting self-assembling (SLSA) raspberry-like AuNP structures,

$$V_{tot} = V_{lgNP} + N_{Ab} (2V_{Ab} + V_{smNP})$$

where V_{lgNP} is the volume of the large (here $D = 60$ nm) AuNP and V_{smNP} is the volume of the small (here $D = 10$ nm) AuNP.

By using the volume of a sphere,

$$D = 2 \times \sqrt[3]{\frac{3V}{4\pi}}$$

the following table can be calculated for the DLS Z_{avg} size increase by adding antibodies to 54.5 nm AuNPs.

N_{Ab}	$D, Ab+LgNP$ (nm)	$D, SLSA$ (nm)
1	54.8	55.2
2	55.1	55.9
10	57.4	61.0

For 60 nm AuNP-Donkey anti-Rabbit IgG (1 Lig/NP), the Z-average increased below the uncertainty of the measurements (values reported are the mean of five measurements with one standard deviation uncertainty), from (55.1 ± 0.7) nm to (55.3 ± 0.3) nm. For 60 nm AuNP-Donkey anti-Rabbit IgG (2 Lig/NP), the Z-average increased from (54.9 ± 0.6) nm to (56.6 ± 0.4) nm. For 60 nm AuNP-Donkey anti-Rabbit IgG (10 Lig/NP), the Z-average increased 4.7 nm from (54.5 ± 0.7) nm to (59.2 ± 1.4) nm.

Discussion of Aggregate/Agglomerate Terminology Selection

The following are quotations of the definitions from the International Standards Organization (ISO), American Society for Testing and Materials (ASTM), and the Organization for Economic Cooperation and Development (OECD) on agglomerates and aggregates when used in nanotechnology.

ISO/TC229 Definitions of Aggregate and Agglomerate[1]

“Aggregate”

Descriptor – strongly bonded or fused particles where specific surface area may be significantly smaller than the sum of calculated specific surface areas of individual components; the physical dimensions of a particle determined by specified measurement conditions. A sample of particles of differing sizes is described by a size distribution.

Agglomerate

Descriptor – collection of loosely bound particles or aggregates or mixtures of the two – resulting external specific surface area is similar to the sum of the specific surface areas of the individual components.”

ASTM Standard E2456 Definitions of Aggregate and Agglomerate [2]

“Agglomerate, n—in nanotechnology, a group of particles held together by relatively weak forces (for example, Van der Waals or capillary), that may break apart into smaller particles upon processing, for example.

Aggregate, n—in nanotechnology, a discrete group of particles in which the various individual components are not easily broken apart, such as in the case of primary particles that are strongly bonded together (for example, fused, sintered, or metallically bonded particles).”

OECD Definitions Clarification [3]

“Aggregate”

Particle comprising strongly bonded or fused particles where the resulting external surface area may be significantly smaller than the sum of calculated surface areas of the individual components. The forces holding an aggregate together are strong forces, for example covalent bonds, or those resulting from sintering or complex physical entanglement. Aggregates are also termed secondary particles and the original source particles are termed primary particles
(³⁰ ISO/TC229, Nanotechnologies Terminology and Definitions for Nano-objects nanoparticle, nanofibre and nanoplate, ISO/TS 27687 ISO Copyright Office, Geneva, 2007, p. 8).

Agglomerate

Collection of loosely bound particles or aggregates or mixtures of the two where the resulting external surface area is similar to the sum of the surface areas of the individual components
(³¹ ISO/TC229, Nanotechnologies Terminology and Definitions for Nano-objects nanoparticle, nanofibre and nanoplate, ISO/TS 27687 ISO Copyright Office, Geneva, 2007, p. 7). For this to be the case all primary particles would need to be at the surface of the agglomerate, which is impossible... a more accurate statement would be “where the surface area measured by gas absorption – BET – is similar to the sum of the surface areas of the individual components.”

Based on these definitions, it is likely that the S-L S-A raspberry-like structures are agglomerates, as the binding between an antibody and an antigen is inherently weak compared to a metal-metal bonds or fused metal nanoparticle cores, and therefore agglomerates is the correct term to use. However, the nature and stability of these agglomerates has not been systematically investigated, beyond AFM imaging showing no

fused metal nanoparticle cores. It is recognized by the authors that the colloidal science community has historically used the term aggregation theory (for example, diffusion limited colloidal aggregation or DLCA, and reaction limited colloidal aggregation or RLCA), which can be used to describe the kinetics of processes that could be defined as either aggregation or agglomeration by these definitions.

References

- [1]. ISO/TC229, Nanotechnologies – Terminology and Definitions for Nano-objects – nanoparticle, nanofibre and nanoplate, ISO/TS 27687 ISO Copyright Office, Geneva, 2007.
- [2]. ASTM Standard E2456 – 06, 2010, “Standard terminology Relating to Nanotechnology,” ASTM International, West Conshohocken, PA, 2010, DOI: 10.1520/E2456-06.
- [3]. OECD Environment, Health and Safety Publications Series on the Safety of Manufactured Nanomaterials, No. 25, Guidance Manual For The Testing Of Manufactured Nanomaterials: OECD Sponsorship Programme, ENV/JM/MONO(2009)20/REV, Organisation for Economic Co-operation and Development, Paris, 2010._page 53

Example AFM Images used to create Figure 3 and 4 histograms

Small to large NP ratios for each raspberry-like structure are labeled on the image. The images selected are intended to be representative of the overall datasets. Predicted small to large NP ratios of 0:1, 1:1, and 2:1 are shown here in Figures SI-2, SI-3, and SI-4, respectively. The antibody autoaffinity positive, which has a predicted small to large NP ratio of 2:1, is shown in Figure SI-5. Note, Figures SI-2 to SI-4 are raw AFM data, while Figure SI-5 has been flattened without any masking, consequently creating the artifact horizontal dark “streaks” near tall particles. Images are 5.00 μm by 5.00 μm , with a Z color scale of 40 nm to enhance visualization of the 10 nm AuNPs. All AFM data was collected using probes with a reported nominal spring constant of 42 N•m⁻¹, a tip radius reported by the vendor equal to or less than 8 nm, and resonant frequency of 330 kHz (NanoAndMore, Lady’s Island, SC)

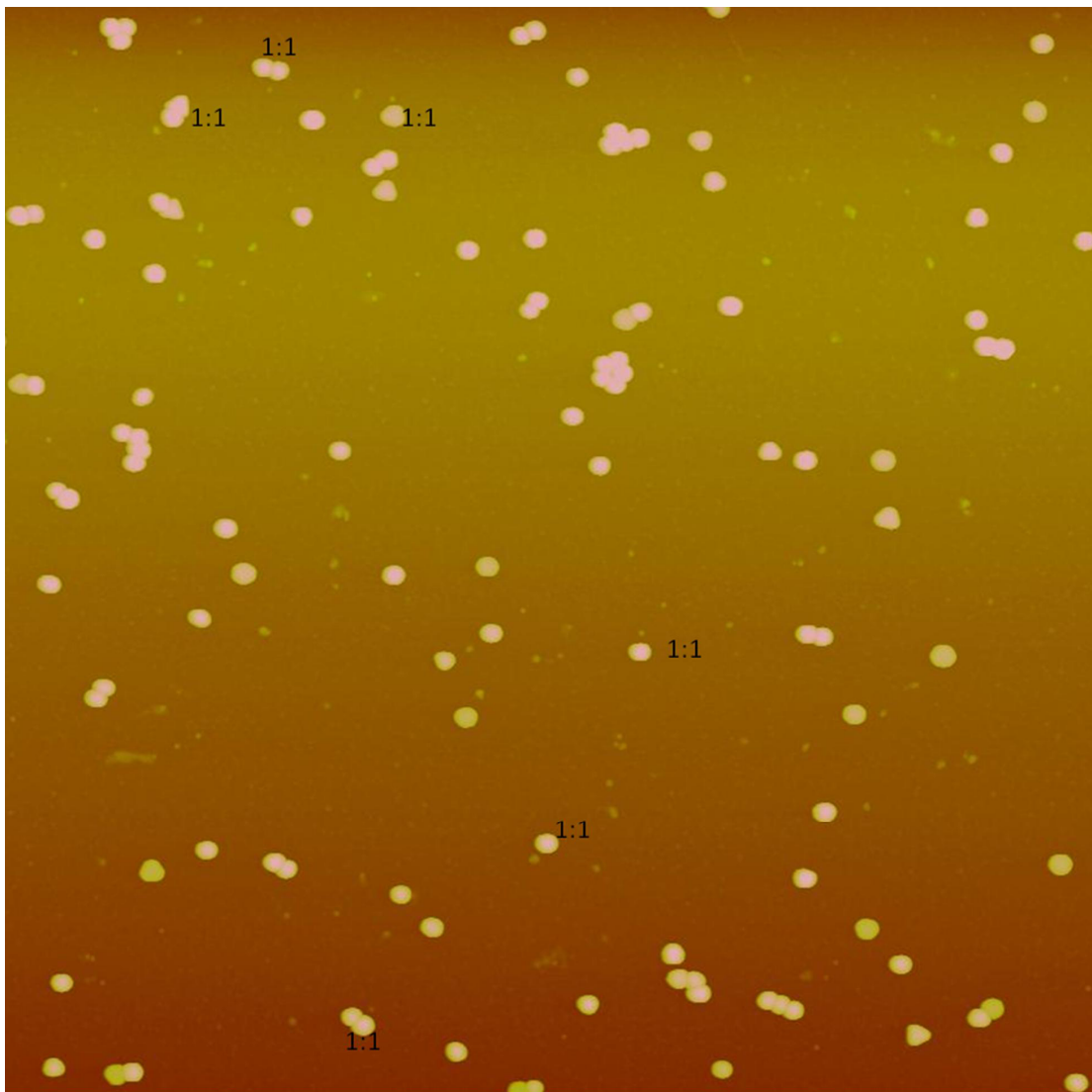


Figure SI-4. Predicted 0:1 Small:Large NP. 0:1 ratios are unlabeled in this image for clarity.

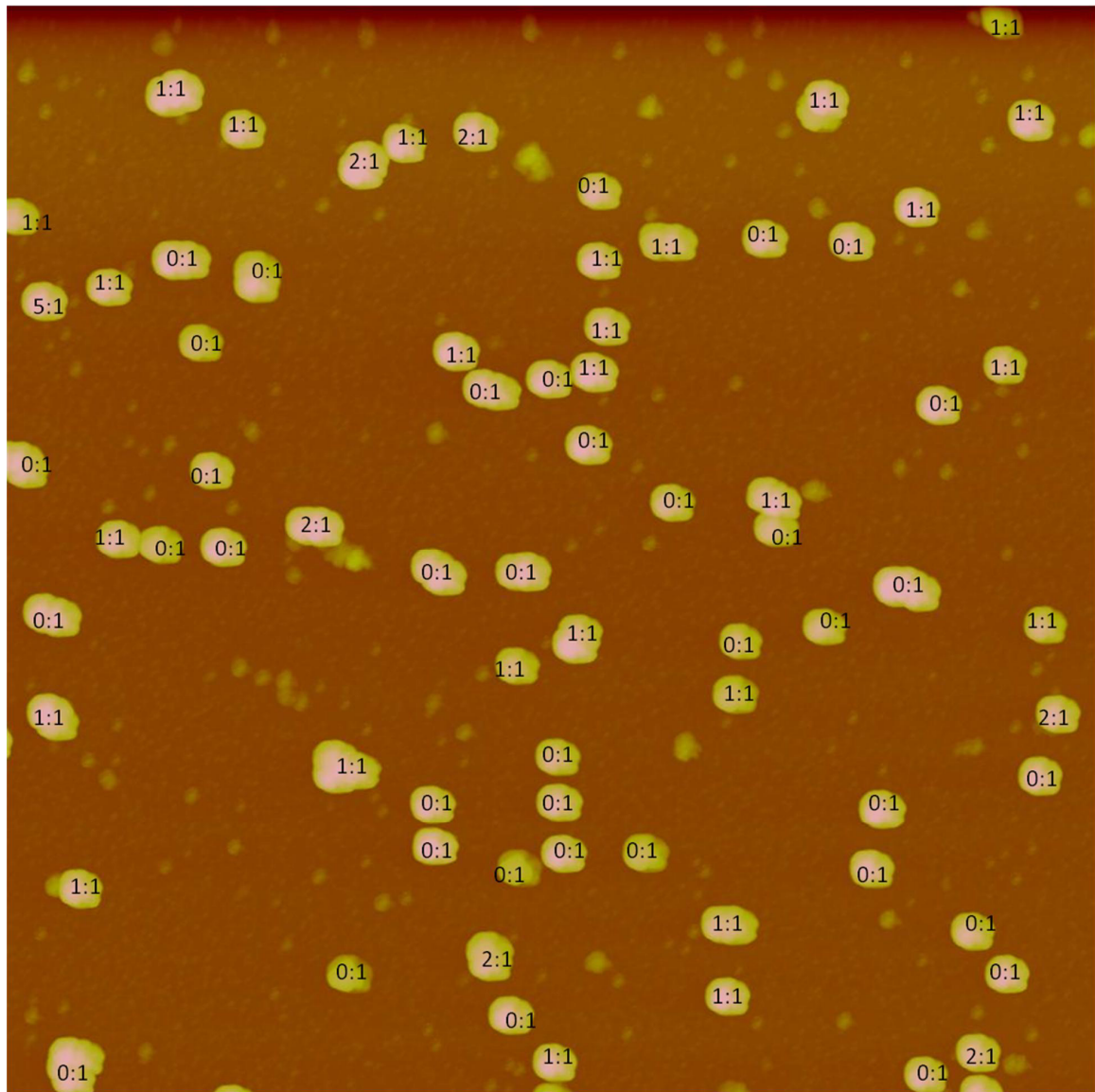


Figure SI-5. Predicted 1:1 Small:Large NP.

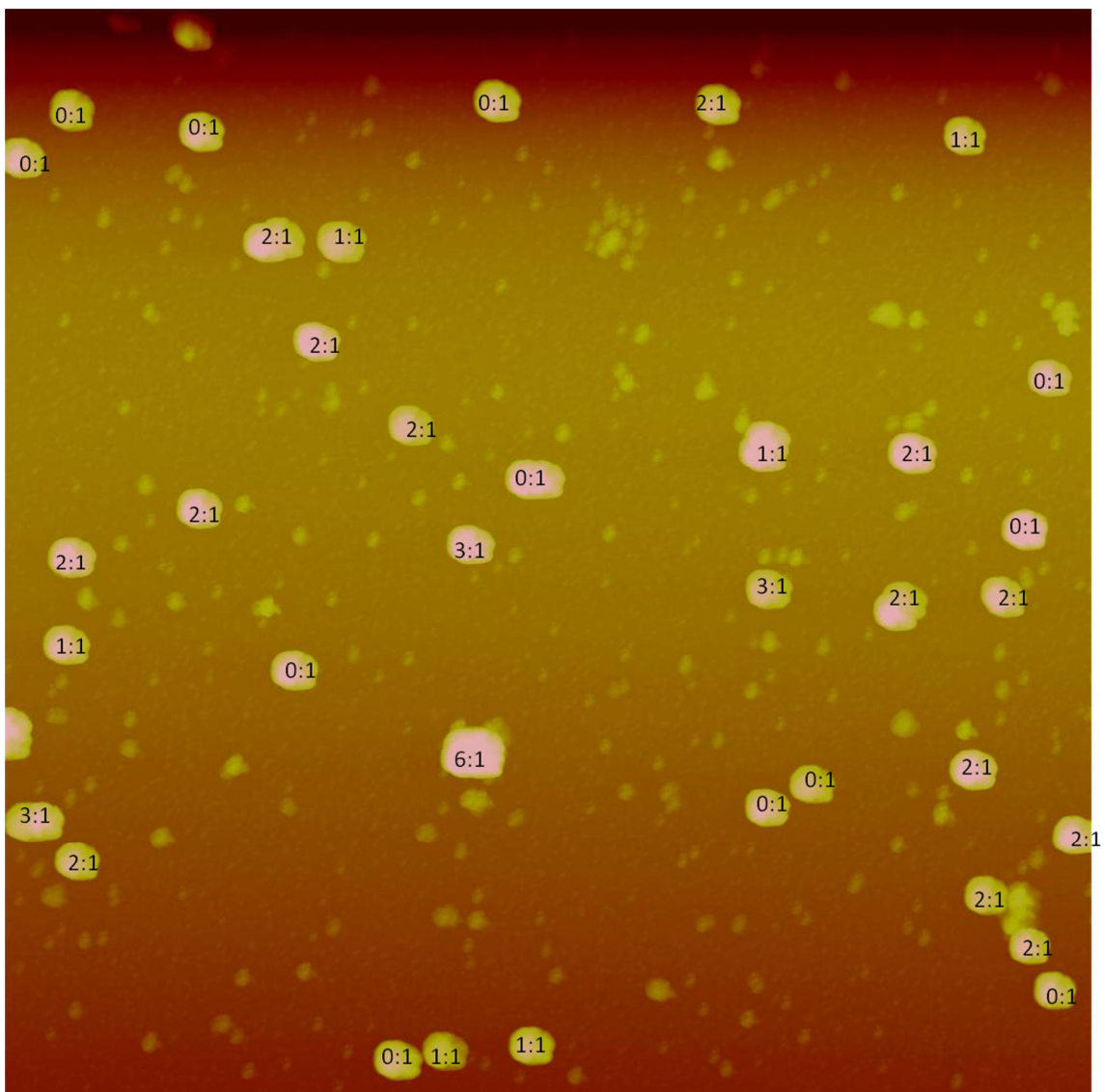


Figure SI-6. Predicted 2:1 Small:Large NP.

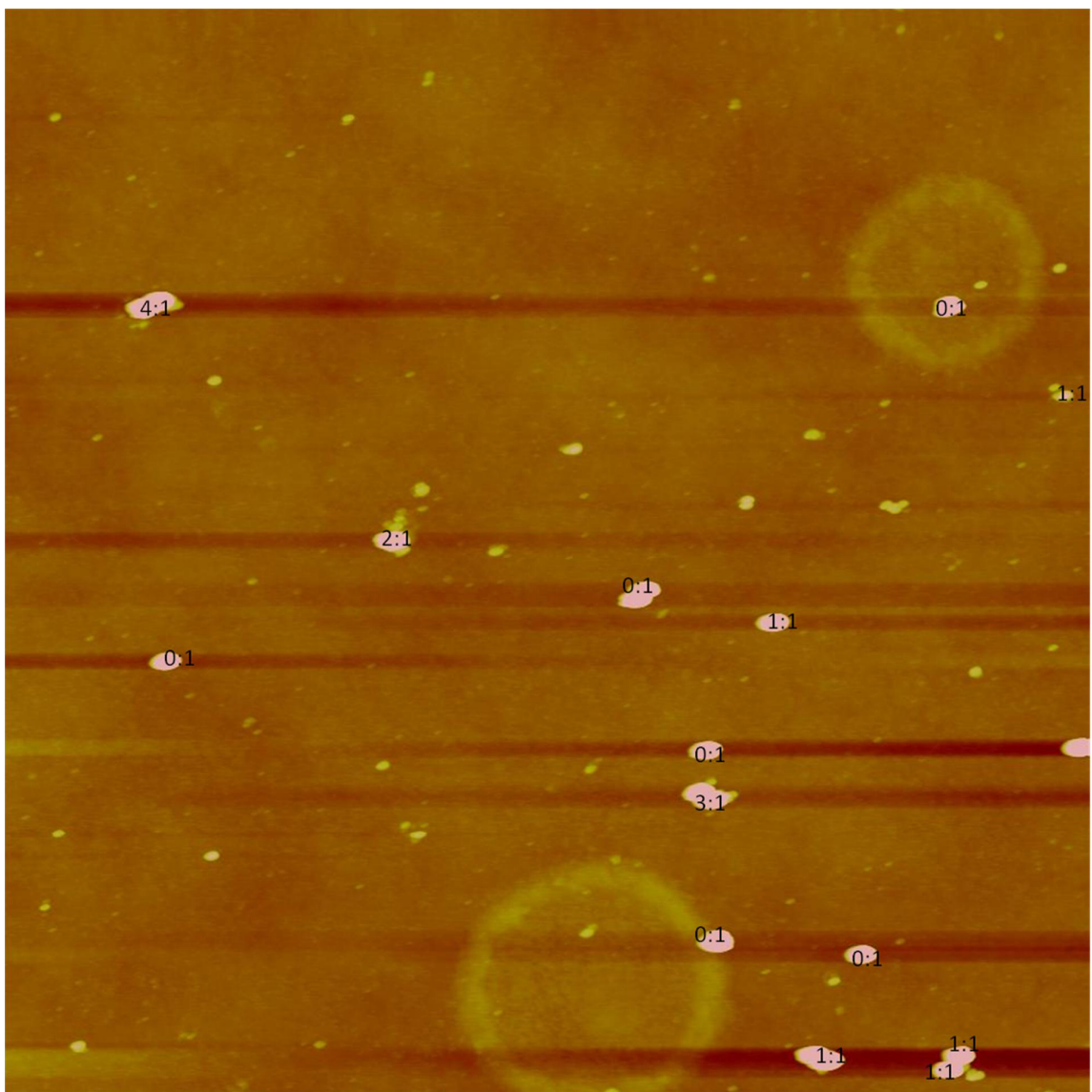


Figure SI-7. Predicted 2:1 Small:Large NP Ab-specificity positive control.

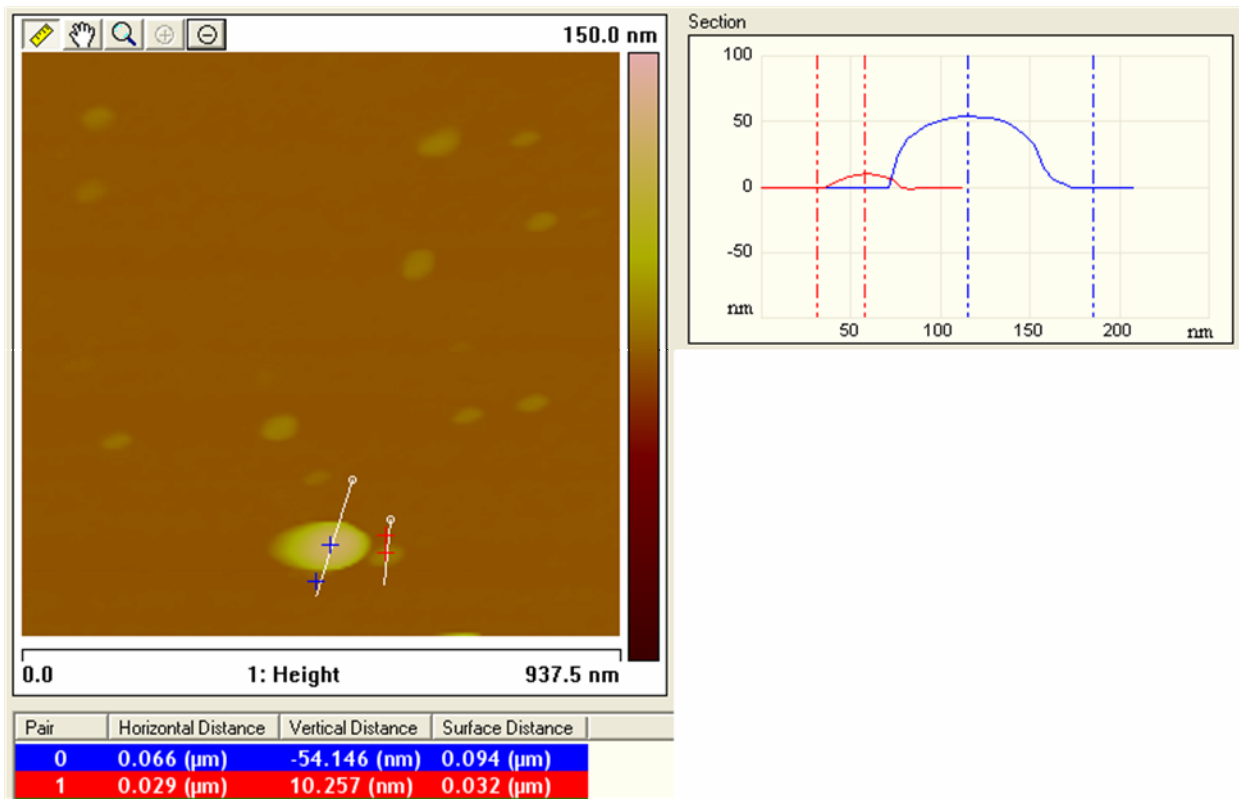


Figure SI-8. Screenshot of cross-section analysis of a 1:1 raspberry-like assembly.